Science Advances
AAAS

Supplementary Materials for

The antiactivator FleN uses an allosteric mechanism to regulate σ^{54}-dependent expression of flagellar genes in *Pseudomonas aeruginosa*

Chanchal, Priyajit Banerjee, Shikha Raghav, Hemant N. Goswami, Deepti Jain*

*Corresponding author. Email: deepti@rcb.res.in

Published 20 October 2021, *Sci. Adv.* **7**, eabj1792 (2021)
DOI: 10.1126/sciadv.abj1792

This PDF file includes:

Figs. S1 to S5

Figure S1

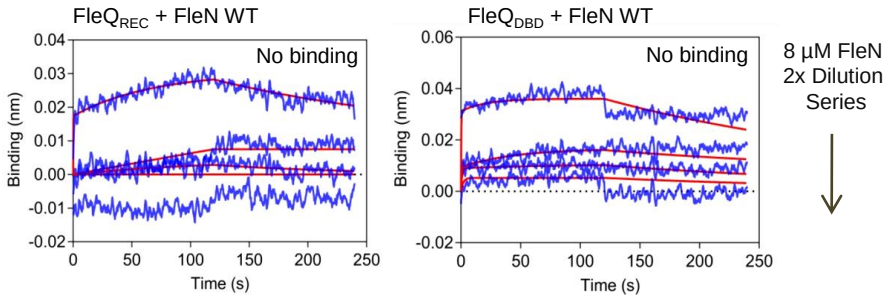

	K_D (µM)	K_{on} (1/Ms)	K_{dis} (1/s)
FleN WT + $FleQ_{REC}$	No binding	No binding	No binding
FleN WT + $FleQ_{DBD}$	No binding	No binding	No binding

Fig. S1 $FleQ_{REC}$ and $FleQ_{DBD}$ interaction with FleN. Biolayer interferometry curves showing binding of $FleQ_{REC}$ and $FleQ_{DBD}$ with FleN WT at different concentrations. The curves in blue and red colours indicate experimental and fitting data respectively. No binding was observed in both the constructs of FleQ.

Figure S2

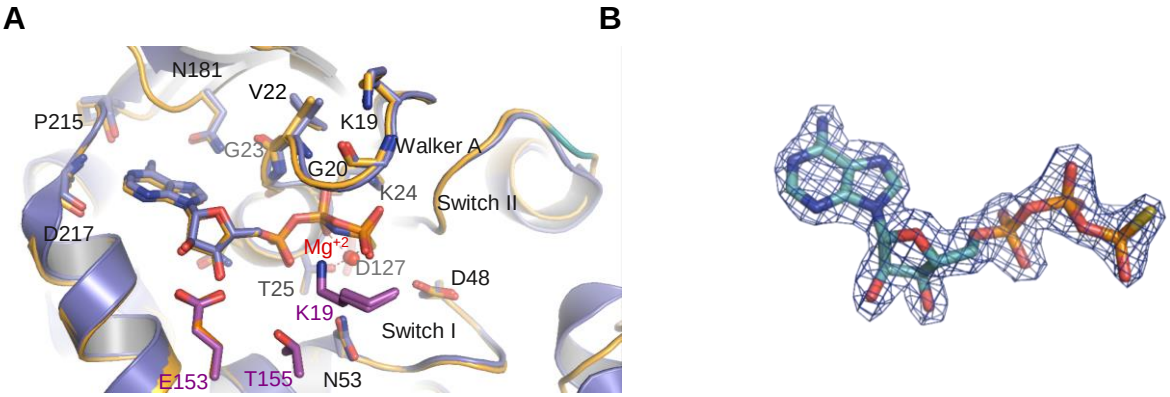

Fig. S2 ATP binding pocket of FleN. (A) Superimposition of ATP binding pocket from FleN-AMPPNP (slate, PDB: 5J1J) and FleN-ATPγS-FleQ$_{AAA+}$ (bright orange) structures. Residues in purple are from the adjacent monomer. **(B)** 2Fo − Fc map at 2.0σ showing ATPγS bound to the FleN in FleN-ATPγS-FleQ$_{AAA+}$ structure.

Figure S3

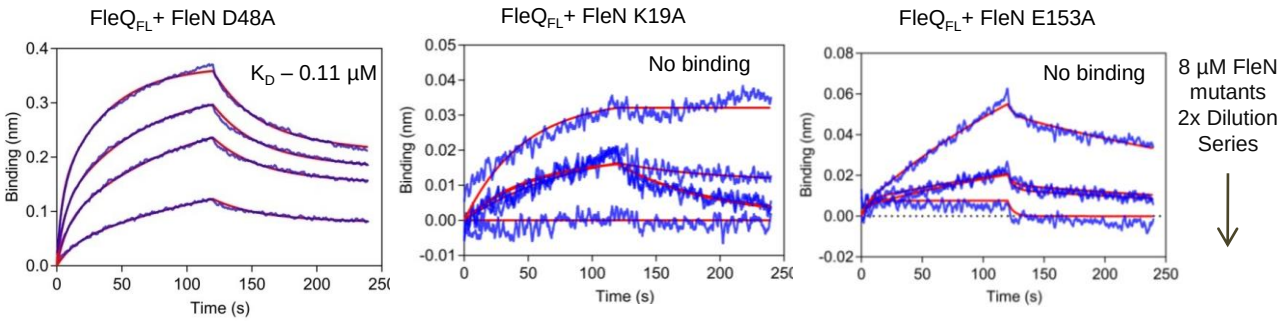

	K_D (µM)	K_{on} (1/Ms)	K_{dis} (1/s)
$FleQ_{FL}$+FleN WT	0.34 ± 0.03	3.65E+03 ± 0.80	1.82E-03 ± 0.94
$FleQ_{FL}$+FleN K19A	No binding	No binding	No binding
$FleQ_{FL}$+FleN E153	No binding	No binding	No binding
$FleQ_{FL}$+FleN D48A	0.11 ± 0.01	7.0E+03 ± 0.08	0.8E-03 ± 0.05

Fig. S3 Interaction between $FleQ_{FL}$ and ATP binding and hydrolysis mutants of FleN. Biolayer Interferometry curves showing interaction between $FleQ_{FL}$ and FleN variants (FleN D48A, FleN K19A and FleN E153A) at different concentrations. The curves in blue and red colours indicate experimental and fitting data respectively. The dissociation constants (K_D, µM), rate of association (K_{on}, 1/Ms) and dissociation (K_{dis}, 1/s) are shown in the table along with standard deviations.

Figure S4

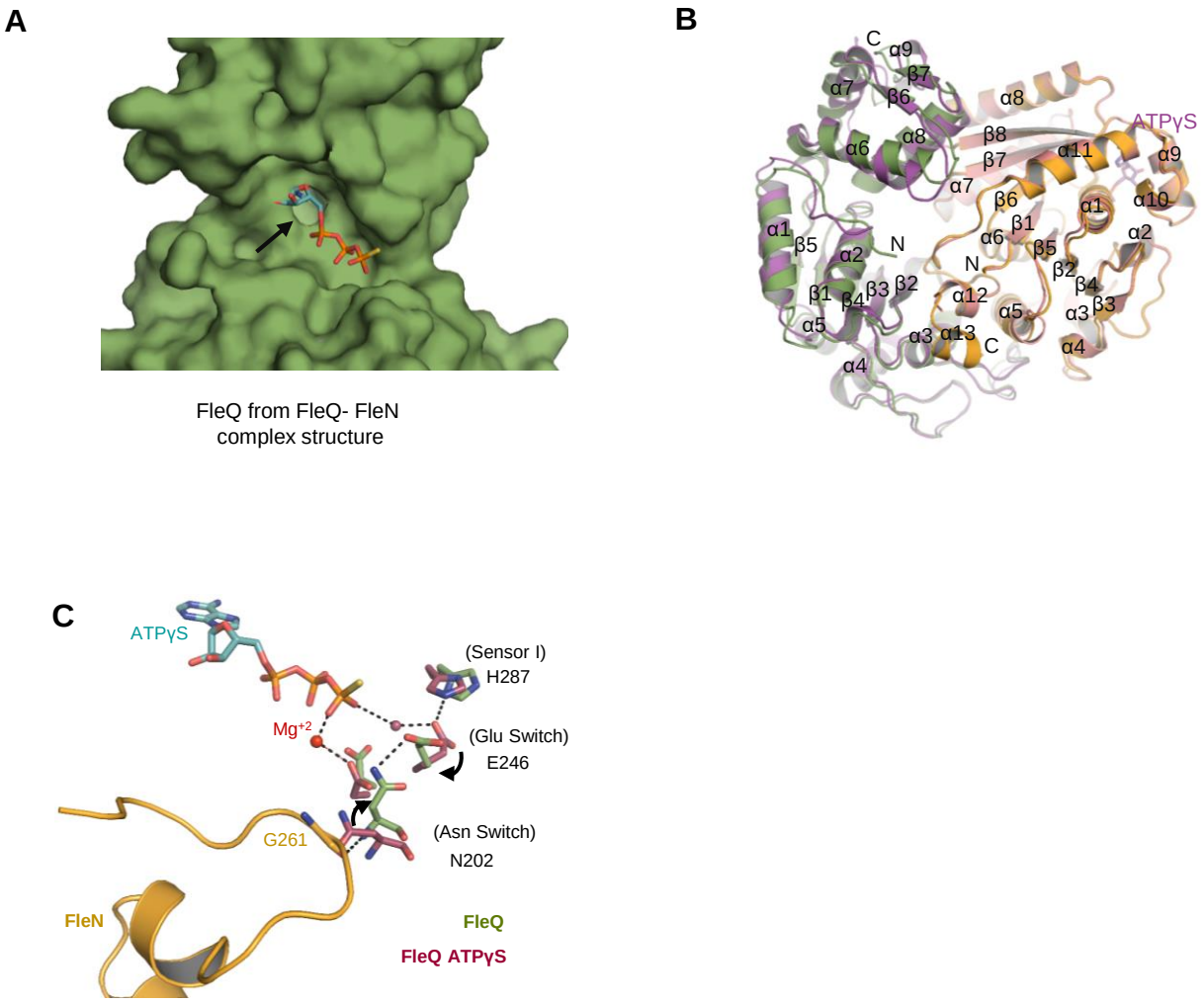

Fig. S4 Superimposition of $FleQ_{AAA+}$ from ATPγS-Mg^{+2} bound and FleN-ATPγS-$FleQ_{AAA+}$ structures. (A) Surface representation of $FleQ_{AAA+}$ in FleN-ATPγS-$FleQ_{AAA+}$ structure (smudge), depicts that the ATP binding pocket (highlighted with black arrow) is too shallow to accommodate ATPγS in it and shows steric clash. **(B)** Superimposition of one half of the complex containing chain A of FleN (bright orange) and $FleQ_{AAA+}$ domain (smudge) on to second half containing chain B of FleN (salmon) and $FleQ_{AAA+}$ domain (purple) showing difference in the α-helical subdomain. **(C)** Superimposition of residues of FleQ from FleN-ATPγS-$FleQ_{AAA+}$ and FleQ-ATPγS structures shows that G261 of FleN (bright orange) sterically clashes with N202 (Asn Switch) in ATPγS bound $FleQ_{AAA+}$ structure.

Figure S5

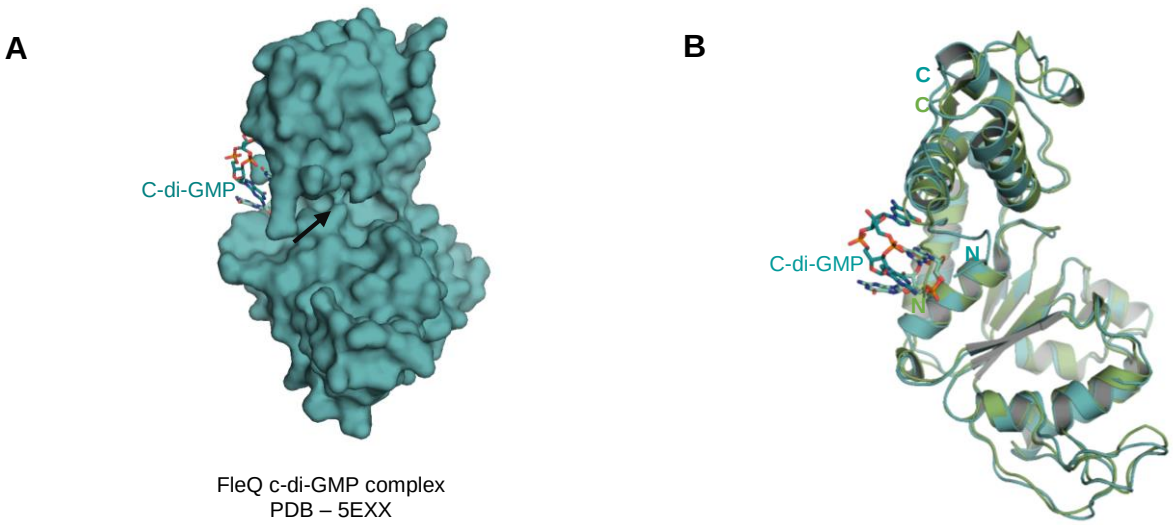

Fig. S5 Structural comparison with c-di-GMP bound structure of $FleQ_{AAA+}$. (A) Surface representation of FleQ-c-di-GMP structure (green cyan, PDB: 5EXX) showing the conformation of ATP binding pocket (black arrow). **(B)** Structural superimposition of $FleQ_{AAA+}$ from c-di-GMP bound (green, PDB: 5EXX) and FleN-ATPγS-$FleQ_{AAA+}$ structures (cyan).